MALAT1 promotes liver fibrosis by sponging miR-181a and activating TLR4-NF-κB signaling

YINGHUI WANG[1*], QIUJU MOU[2*], ZIXIN ZHU[3], LUQIANG ZHAO[1,2] and LILI ZHU[1,2]

[1]School of Clinical Laboratory Science, Guizhou Medical University; [2]Department of Blood Transfusion, The Affiliated Hospital of Guizhou Medical University, Guiyang, Guizhou 550004; [3]Department of Basic Medical College, Guizhou Medical University, Guiyang, Guizhou 550025, P.R. China

Received September 16, 2020; Accepted September 9, 2021

DOI: 10.3892/ijmm.2021.5048

Abstract. The aim of the present study was to investigate whether long non-coding RNA metastasis associated lung adenocarcinoma transcript 1 (MALAT1) could modulate activation and inflammation of hepatic stellate cell (HSCs) via regulation of a microRNA (miR)-181a-toll like receptor (TLR)4/nuclear factor (NF)-κB axis, thereby contributing to the development of liver fibrosis. A total of 151 patients with liver fibrosis were recruited, and the serum levels of alanine transaminase, aspartate aminotransferase and albumin were determined. Transforming growth factor (TGF)-β1 and LPS were used to activate and induce inflammation in the human HSC cell line LX2. MALAT1 was knocked using small interfering RNA or overexpressed, and an inhibitor and mimic of miR-181a-5p were used to examine the effect of MALAT1 and miR-181a-5p on the activation and inflammation of LX2 cells. Both MALAT1 and miR-181a-5p expression performed well in their ability to differentiate patients with liver fibrosis from healthy volunteers, and MALAT1 expression was associated with the severity of liver fibrosis. The expression levels of TLR4 and NF-κB were increased after stimulation with LPS or TGF-β1, but MALAT1 knockdown or miR-181a-5p mimic transfection abrogated this increase. Moreover, the TGF-β1-induced increase in viability, proliferation, migration, adhesion and collagen production, and the LPS-induced inflammation of LX2 cells were all reversed after MALAT1 knockdown or transfection with miR-181a-5p mimic. The MALAT1/miR-181a-5p axis was involved in regulating collagen production and inflammation by activating TLR4/NF-κB signaling, which may be conducive to liver fibrosis treatment in the future.

Correspondence to: Dr Lili Zhu, Department of Blood Transfusion, The Affiliated Hospital of Guizhou Medical University, 28 Guiyi Street, Yunyan, Guiyang, Guizhou 550004, P.R. China
E-mail: zhulili_guizhou@126.com

*Contributed equally

Key words: liver fibrosis, long non-coding RNA metastasis associated lung adenocarcinoma transcript 1, microRNA-181a-5p, lipopolysaccharide, transforming growth factor-β1, inflammation, collagen production, diagnosis

Introduction

Despite accounting for only a small percentage (5-8%) of liver cells, hepatic stellate cells (HSCs) are important for liver cell regeneration and development of liver fibrosis (1,2). Specifically, liver injuries facilitate the release of cytokines such as tumor necrosis factor-α (TNF-α) and transforming growth factor-β (TGF-β) from hepatocytes and Kupffer cells, as well as the release of reactive oxygen species (ROS), causing resting HSCs to transform into α-smooth muscle actin (α-SMA)-expressing myofibroblast-like cells. As a consequence, HSCs proliferate aggressively and produce large quantities of extracellular matrix proteins, primarily collagen, which ultimately leads to liver fibrosis (3,4). Liver fibrosis treatment is often delayed, and there is a high incidence of liver cancer in patients with liver fibrosis (5). It is therefore crucial to understand the mechanisms of HSC activation and inflammation, in order to develop novel diagnostic and treatment strategies for liver fibrosis.

Extensive research underlines the link between long non-coding RNAs (lncRNAs) and liver fibrosis development, suggesting that lncRNAs have potential value in diagnosis, prognosis and treatment of liver fibrosis (6). For example, lncRNA H19 and liver fibrosis-associated lncRNA were reported to accelerate or decelerate liver fibrosis progression, respectively, by altering TGF-β1/Smad signaling and collagen production (7-10). Furthermore, lncRNA metastasis associated lung adenocarcinoma transcript 1 (MALAT1), also known as nuclear enriched abundant transcript 2, was reported to be a negative regulator of sirutin 1 (11), upregulated expression of which induces Smad3 deacetylation and deactivation of HSC (12). MALAT1 also promotes HSC activation by targeting microRNA (miR/miRNA)-101b and increasing Rac1 expression (13), and increasing collagen 1 (COL1)A2 expression by downregulating miR-26b (14). miR-181a, although sponged by MALAT1 in myeloma cells (15), was reported to rescue the aberrant inflammatory cascade and over-proliferation of HSCs by decreasing TLR4/NF-κB signaling, thereby limiting liver fibrosis progression (16,17). However, there

is no convincing evidence suggesting a role for the lncRNA MALAT1/miR-181a axis in the etiology of liver fibrosis, to the best of our knowledge. Therefore, the aim of the present study was to elucidate the contribution of the MALAT1/miR-181a axis in the abnormal inflammation and HSC activation underlying the pathogenesis of liver fibrosis.

Materials and methods

Clinical samples. In total, 151 patients with liver fibrosis or chronic hepatitis B virus (HBV)-associated liver fibrosis were recruited at the Affiliated Hospital of Guizhou Medical University (Guiyang, China), between October 2018 and December 2019. The age range of the patient cohort was 25-68 years, with a median age of 51. The cohort consisted of 116 males and 35 females. The inclusion criteria were: i) Liver fibrosis was histopathologically confirmed (Fig. S1); ii) Hepatitis B antigen remained positive for >6 months; iii) HBV DNA was ≥105 IU/ml; iv) alanine aminotransferase (ALT) levels were ~1 fold higher than the normal range; and v) patients were fully informed about this program. The present study was approved by the Ethics Committee of the Affiliated Hospital of Guizhou Medical University. Conversely, participants were excluded if: i) They were infected with hepatitis C virus, hepatitis A virus, hepatitis D virus or other hepatotropic viruses; ii) their livers were damaged due to alcohol or drug use, or immune disorders; iii) they had diabetes, hypertension, malignant tumors or any other severe lesions in the heart, kidneys or lungs; iv) they received anti-viral treatment within the preceding 6 months; or v) they suffered from acute HBV infection, liver failure or cirrhosis. Concurrently, 93 healthy individuals without a family history of HBV and with normal liver function were recruited as controls. The age range of control group was 22-73, with a median age of 46, consisting of 67 males and 26 females. Written informed consent was obtained from all participants included in the present study.

Venous blood was taken from the medical cubital vein of each subject on an empty stomach, and serum levels of ALT, aspartate aminotransferase (AST) and albumin were determined using an automatic biochemical analyzer (model: 7600P, Hitachi, Ltd.), according to the manufacturer's protocol (Beijing Solarbio Science & Technology Co., Ltd.). Serum levels of hyaluronic acid (HA), procollagen III (PC-III), collagen type IV (C-IV) and laminin (LN) were detected by chemiluminescence immunoassay (CL-2000I; Mindray Medical International, Ltd.). Serum levels of tumor necrosis factor-α (TNF-α), interleukin-6 (IL-6) and high-sensitivity C-reactive protein (hs-CRP) were determined using specific ELISA kits (cat. nos. 1749-48T, A100084-96T and A099284-96T; Affandi-e).

Cell culture. The human LX2 HSC cell line (Shanghai Advanced Research Institute, The Cell Bank of Type Culture Collection of The Chinese Academy of Sciences) was cultured in DMEM with 2% FBS in a humidified incubator at 37˚C incubator supplied with 5% CO_2.

Cell treatment with TGF-β1 or LPS. LX2 cells were treated with recombinant human TGF-β1 (PeproTech, Inc.) at 5, 10 and 15 ng/ml for 24 h, as described previously (18). LX2 cells were treated with LPS (Sigma-Aldrich; Merck KGaA) at a final concentrations of 0.01, 0.1 and 1 μg/ml for 24 h.

Cell transfection. LX2 cells in the logarithmic growth phase, were seeded at a density of $6x10^5$ cells/well, were separately transfected with pcDNA3.1-MALAT1, small interfering (si) RNA against MALAT1-1 (si-MALAT1-1), si-MALAT1-2 miR-181a-5p mimic or miR-181a-5p inhibitor (all synthesized by Shanghai GenePharma, Co., Ltd.) for 48 h, using Lipofectamine 2000 according to the manufacturer's protocol (Invitrogen; Thermo Fisher Scientific, Inc.). The working concentration of plasmids was 100 nM. The sequences of the constructs used were: si-MALAT1-1: 5'-CCUCAGACAGGU AUCUCUU-3'; si-MALAT1-2 5'-GAUCCAUAAUCGGUU UCAA-3'; miR-181a-5p mimic, 5'-AACAUUCAACGCUGU CGGUGAGU-3' and 3'-UUGUAAGUUGCGACAGCCACU CA-5'; miR-mimic NC, 5'-UUUGUACUACACAAAAGU ACUG-3' and 3'-AAACAUGAUGUGUUUUCAUGAC-5'; miR-181a-5p inhibitor 5'-ACUCACCGACAGCGUUGAAUG UU-3'; and miR-inhibitor NC 5'-CAGUACUUUUGUGUA GUACAAA-3'.

MTT assay. LX2 cells were seeded into 96-well plates at a density of $4x10^3$ cells/well. Once they had adhered to the plate, 20 μl MTT (5 mg/ml) was added for 4 h. Subsequently, 150 μl DMSO (Sinopharm Chemical Reagent Co., Ltd.) was added to each well, and the mixture was shaken at 37˚C for 10 min. Absorbance was measured on a microplate reader (Elx800, BioTek Instruments Inc.) at 490 nm.

Transwell assays. LX2 cells were resuspended in serum-free medium ($1x10^5$ cells/ml) and seeded in the upper chamber of 24-well plate Transwell inserts (Corning, Inc.). A total of 500 μl supplemented medium was added to the lower chamber. After 24 h of incubation, the polycarbonate membranes and the cells remaining in the upper chamber were removed, and the chambers were immersed in crystal violet solution (Merck KGaA) for 10 min at 37˚C, until cells in the lower chamber were dyed violet.

Wound healing assay. LX2 cells were seeded into 6-well plates and cultured until 80% confluent. Culture medium was replaced with serum-free medium and the cell layer was scratched using a 200 μl pipette tip, along the center of the wells. After 24 h, images of the culture plates were taken using a light microscope. (magnification, x200).

Flow cytometry. After centrifugation at 42.62 x g for 5 min at room temperature, LX2 cells were re-suspended in 1X binding buffer at a density of $1x\ 10^6$/ml. A total of 5 μl Annexin V/FITC and 5 μl propidium iodide (BD Biosciences) were added to 100 μl cell suspension, followed by incubation in the dark at room temperature for 15 min. The proportion of apoptotic cells was determined by flow cytometry (Coulter epics-XL; Beckman Coulter, Inc.) and analyzed using CellQuest version 3.2 software (BD Bioscience).

Colony formation assay. LX2 cells ($2x10^3$ cells/well) were seeded in 6-well plates and cultured at 37˚C in 5% CO_2

for 12 days. Cells were fixed using 4% paraformaldehyde (Wuhan Boster Biological Technology, Ltd.) for 20 min and then stained with 1% crystal violet (Wuhan Boster Biological Technology, Ltd.) for 20 min, both at room temperature. Colonies consisting of >50 cells were counted manually under a microscope (magnification, x20; BioTek Instruments, Inc.).

Reverse transcription-quantitative (q)PCR. Total RNA was extracted from blood samples of participants and LX2 cells using an easyPureBlood RNA kit (TransGen Biotech, Co. Ltd.). RNA was reverse transcribed into cDNA using a HiScript III 1st Strand cDNA Synthesis kit (Biotech Co., Ltd.) according to the manufacturer's protocol, after which qPCR was performed using SYBR-Green (Roche Diagnostics), with the following thermocycling parameters: 95˚C for 15 min; followed by 40 cycles of 94˚C for 15 sec and 55˚C for 30 sec; and a final extension step of 70˚C for 60 sec. The primer sequences used are listed in Table SI. Expression of MALAT1 and miR-181a-5p were normalized to GAPDH or U6, respectively, using the $2^{-\Delta\Delta Cq}$ method (19).

Western blotting. Proteins (50 μg), extracted from blood samples and LX2 cells using a protein extraction kit according to the manufacturer's protocol (Applygen Technologies Inc.), were loaded on a 10% SDS-gel, resolved using SDS-PAGE and then transferred to PVDF membranes. The protein concentration was determined using a BCA protein assay kit (Beyotime Institute of Biotechnology). After blocking with 5% skimmed milk powder for 1.5 h at room temperature, the protein samples were incubated with primary antibodies against NF-κB (1:1,000; cat. no. 8242; Cell Signaling Technology, Inc.), toll like receptor (TLR) 4 (1:500; cat. no. ab13556; Abcam), α-SMA (1:1,000; cat. no. 19245; Cell Signaling Technology, Inc.), COL1 (1:100; cat. no. 72026; Cell Signaling Technology, Inc.), tissue inhibitor of metalloprotease (TIMP)-1 (1:1,000; cat. no. ab211926; Abcam), Bax (1:2,000; cat. no. ab32503; Abcam), Bcl-2 (1:1,000; cat. no. ab32124; Abcam), cleaved caspase-3 (1:500; cat. no. ab2302; Abcam), E-cadherin (1:25; cat. no. ab227639; Abcam), Desmin (1:1,000; cat. no. ab227224; Abcam), Vimentin (1:2,000; cat. no. ab92547; Abcam) and GAPDH (1:2,500; cat. no. ab9485; Abcam) at 4˚C overnight, and were then incubated with HRP-conjugated goat anti-rabbit IgG (1:3,000; cat. no. ab6721; Abcam) for 1 h at room temperature. Following chemiluminescent detection, protein bands were quantified using the Gel-pro software (version 3.1; Media Cybernetics, Inc.).

Dual-luciferase reporter gene assay. MALAT1 fragments that incorporated binding sites for miR-181a-5p were amplified using PCR and cloned into a pmirGLO vector (Promega Corporation). These were then mutated to remove the predicted miR-181a-5p binding sites using site-directed mutagenesis to construct a plasmid termed pmiRGLO-MALAT1-Mut. pmirGLO-MALAT1-Wt or pmirGLO-MALAT1-Mut were co-transfected with miR-181a-5p mimic or miR-NC into LX2 cells using Lipofectamine 2000, according to the manufacturer's protocol (Invitrogen; Thermo Fisher Scientific, Inc.). Renilla and firefly luciferase activities were detected using a dual-luciferase reporter assay system, according to the manufacturer's protocol (Promega Corporation).

RNA immunoprecipitation (RIP) assay. RIP from LX2 cells was performed using a Magna RIP™ RNA-Binding Protein Immunoprecipitation kit (MilliporeSigma), and cell lysates were incubated with RIP buffer containing magnetic beads conjugated with human anti-Ago2 antibody (MilliporeSigma) or IgG (MilliporeSigma) at 4˚C overnight. The resulting protein-RNA complexes were digested with proteinase K to release RNA, which was then qualified by RT-qPCR as described above.

Fluorescence in situ hybridization (FISH) for MALAT1 and miR-181a-5p in LX2 cells. RNA FISH assays were performed using a FISH kit (Creative Bioarray) according to the manufacturer's protocol. LX2 cells were incubated with 0.2 mol/l HCl and 0.3% Triton X-100 at room temperature. After fixing cells with 4% formaldehyde at room temperature for 10 min, RNA hybridization buffer was added to the cells, and pre-hybridization was performed at 55˚C for 2 h. Subsequently, RNA probes, having been denatured at 85˚C for 5 min and 37˚C for 2 min, were added and hybridization was performed in the dark at 37˚C overnight. The length of MALAT1 probe is 20 bp, and the sequence is 5'-TATGACACTTTCCTTGCCCA-3'. The length of the miR-181a-5p probe is 23 nt, and the sequence is 5'-TTGTTTGTTGCGTCTGCCTCTCT-3' with 23 bp. Images were collected on a confocal laser scanning microscope (magnification: x600; FV1000; Olympus Corporation).

Statistical analysis. All data were statistically analyzed using SPSS version 22.0 (IBM, Corp.). Continuous data (mean ± standard deviation) were compared between groups using an unpaired Student's t-test, and count data were compared using a χ^2 test. Pearson's correlation coefficients were calculated to assess correlations between serum levels of lncRNA MALAT1, miR-181a-5p, inflammatory factors and hepatic fibrosis indices, as well as receiver operating characteristic (ROC) curves were constructed to evaluate the diagnostic value of lncRNA MALAT1 and miR-181a-5p for patients with liver fibrosis. $P<0.05$ was considered to indicate a statistically significant difference.

Results

Clinical significance of lncRNA MALAT1 and miR-181a-5p in liver fibrosis. Patients with liver fibrosis had higher serum levels of ALT and AST and lower serum levels of albumin than the healthy volunteers, and the two populations did not have significantly different mean ages or sex ratios ($P>0.05$; Table I). Serum levels of inflammatory factors, including TNF-α, IL-6 and hs-CRP, as well as liver fibrosis indicators, including HA, PC-III, C-IV and LN, were higher in patients with liver fibrosis compared with the healthy controls ($P<0.05$). Furthermore, the levels of MALAT1 in the serum of patients with liver fibrosis was ~2X higher than that in the healthy subjects ($P<0.05$), whereas serum miR-181a-5p levels were significantly reduced in patients with liver fibrosis relative to the healthy controls ($P<0.05$; Fig. 1A). MALAT1 and miR-181a-5p expression levels were positively and negatively correlated, respectively, with the severity of liver fibrosis (Fig. 1B). It was noteworthy that both serum MALAT1 and miR-181a-5p had high area under ROC curve (AUC) values

Table I. Comparison of baseline features between patients with liver fibrosis and healthy volunteers.

Characteristics	Patients	Healthy control	χ^2/t	P-value
Age, year	43.96±10.35	43.58±11.29	0.27[c]	0.788
Sex			6.94[d]	0.008[a]
Male	116	67		
Female	35	26		
Stage				
F0-F1	40	-	-	-
F2-F3	62	-	-	-
F4	49	-	-	-
Alanine transaminase, μg/l	35.91±16.74	14.71±7.52	11.51[c]	<0.001[b]
Aspartate aminotransferase, μg/l	51.45±18.31	17.65±5.36	17.34[c]	<0.001[b]
Albumin, g/l	45.26±16.82	76.38±4.05	17.52[c]	<0.001[b]
HBV-DNA, $\log_{10}$ copies/ml	5.25±1.83	-	-	-
Tumor necrosis factor-α, ng/l	263.56±39.15	96.89±18.8	38.40[c]	<0.001[b]
Interleukin-6, ng/l	283.51±48.17	53.28±12.64	45.11[c]	<0.001[b]
High-sensitivity C-reactive protein, ng/l	349.34±52.14	66.25±19.52	50.20[c]	<0.001[b]
Serum hyaluronic acid, μg/l	106.34±31.47	15.06±4.63	27.77[c]	<0.001[b]
Procollagen III, μg/l	35.49±18.78	3.41±1.85	15.93[c]	<0.001[b]
Collagen type IV, μg/l	32.22±17.24	6.53±3.29	13.30[c]	<0.001[b]
Laminin, μg/l	10.17±2.44	3.31±1.12	25.49[c]	<0.001[b]

[a]P<0.01, [b]P<0.001. [c]Analyzed using a χ^2 test. [d]Analyzed using an unpaired t-test.

of 0.901 and 0.944, respectively, suggesting that they may be useful for diagnosis of liver fibrosis. MALAT1 in combination with miR-181a-5p resulted in an even higher AUC value, 0.984 (Fig. 1C; Table II).

Serum levels of MALAT1 were negatively correlated with serum levels of miR-181a-5p in the patients with liver fibrosis (r_s=-0.463; Fig. 2A). MALAT1 was positively correlated with serum TNF-α (r_s=0.454), IL-6 (r_s=0.351) and hs-CRP (r_s=0.341), whereas serum miR-181a-5p levels were negatively correlated with TNF-α (r_s=-0.340), IL-6 (r_s=-0.358) and hs-CRP (r_s=-0.333) (Fig. 2B). Serum levels of the liver fibrosis indicators HA, PC-III, C-IV and LN were positively correlated with serum MALAT1 (HA, r_s=0.399; PC-III, r_s=0.361; C-IV, r_s=0.418; LN, r_s=0.451), and negatively correlated with serum miR-181a-5p levels (HA, r_s=-0.405; PC-III, r_s=-0.328; C-IV, r_s=-0.344; LN, r_s=-0.370) (Fig. 2C).

MALAT1 and miR-181a-5p regulate the inflammatory response of HSCs. FISH data (Fig. S2) suggested that MALAT1 (red fluorescence) and miR-181a-5p (green fluorescence) were co-localized in LX2 cells. MALAT1 was primarily localized to the nucleus, whereas miR-181a-5p was present both in the nucleus and the cytoplasm.

Upon stimulation with 0.01, 0.1 and 1 μg/ml LPS, MALAT1 expression in the LX2 cells increased (P<0.05), whereas miR-181a-5p expression decreased (P<0.05; Fig. 3A). MALAT1 expression in LX2 cells was increased after transfection of pcDNA3.1-MALAT1 (P<0.05), and both si-MALAT1-1 and si-MALAT1-2 transfection, significantly decreased MALAT1 expression (P<0.05). miR-181a-5p expression in LX2 cells increased when miR-181a-5p mimics were transfected (P<0.05), and decreased when miR-181a-5p inhibitor was transfected (P<0.05; Fig. 3B).

Expression levels of TLR4 and NF-κB were increased in LX2 cells after LPS exposure (P<0.05) (Fig. 3C). TLR4 and NF-κB were both downregulated in the LPS+si-MALAT1 and LPS+miR-181a-5p mimic group, yet were upregulated in the LPS+pcDNA3.1-MALAT1 and LPS+miR-181a-5p inhibitor group, when compared with the LPS group (P<0.05; Fig. 3C and D). IL-6, IL-1β and TNF-α levels in LX2 cells were increased in the LPS group compared to the control group (P<0.05; Fig. 3E). Levels of these cytokines were increased in the LPS+pcDNA3.1-MALAT1 and LPS+miR-181a-5p inhibitor group, and were decreased in the LPS+si-MALAT1 and LPS+miR-181a-5p mimic group compared with the LPS group (P<0.05; Fig. 3E).

MALAT1 sponges miR-181a-5p and activates TLR4/NF-κB signaling in HSCs. Using RIP assays with an anti-Ago2 antibody, it was shown that MALAT1 interacted with Ago2, a vital constituent of the RNA-induced silencing complex (Fig. 4A). Furthermore, luciferase activity of LX2 cells transfected with pmirGLO-MALAT1-Wt+miR-181a-5p mimics was significantly reduced compared with both pmirGLO-MALAT1-Wt+miR-NC and pmirGLO+miR-181a-5p mimics (both P<0.05; Fig. 4B), suggesting that miR-181a-5p was sponged by MALAT1 in LX2 cells.

Furthermore, miR-181a-5p expression was decreased in LX2 cells transfected with pcDNA3.1-MALAT1 compared with the pcDNA3.1 control (P<0.05), whereas miR-181a-5p expression was increased in cells transfected with si-MALAT1 compared to the si-NC control (P<0.05; Fig. 4C). Expression

Table II. Diagnostic potential of lncRNA MALAT1 and miR-181-5p for liver fibrosis.

Biomarkers	Value	Sensitivity	Specificity	Area under the curve	95% confidence interval
lncRNA MALAT1	2.81	0.781	0.968	0.901	0.862-0.941
microRNA-181-5p	2.62	0.967	0.806	0.944	0.912-0.976
lncRNA MALAT1 and miR-181-5p	-	0.914	0.968	0.984	0.973-0.995

Long-non-coding RNA metastasis associated lung adenocarcinoma transcript 1.

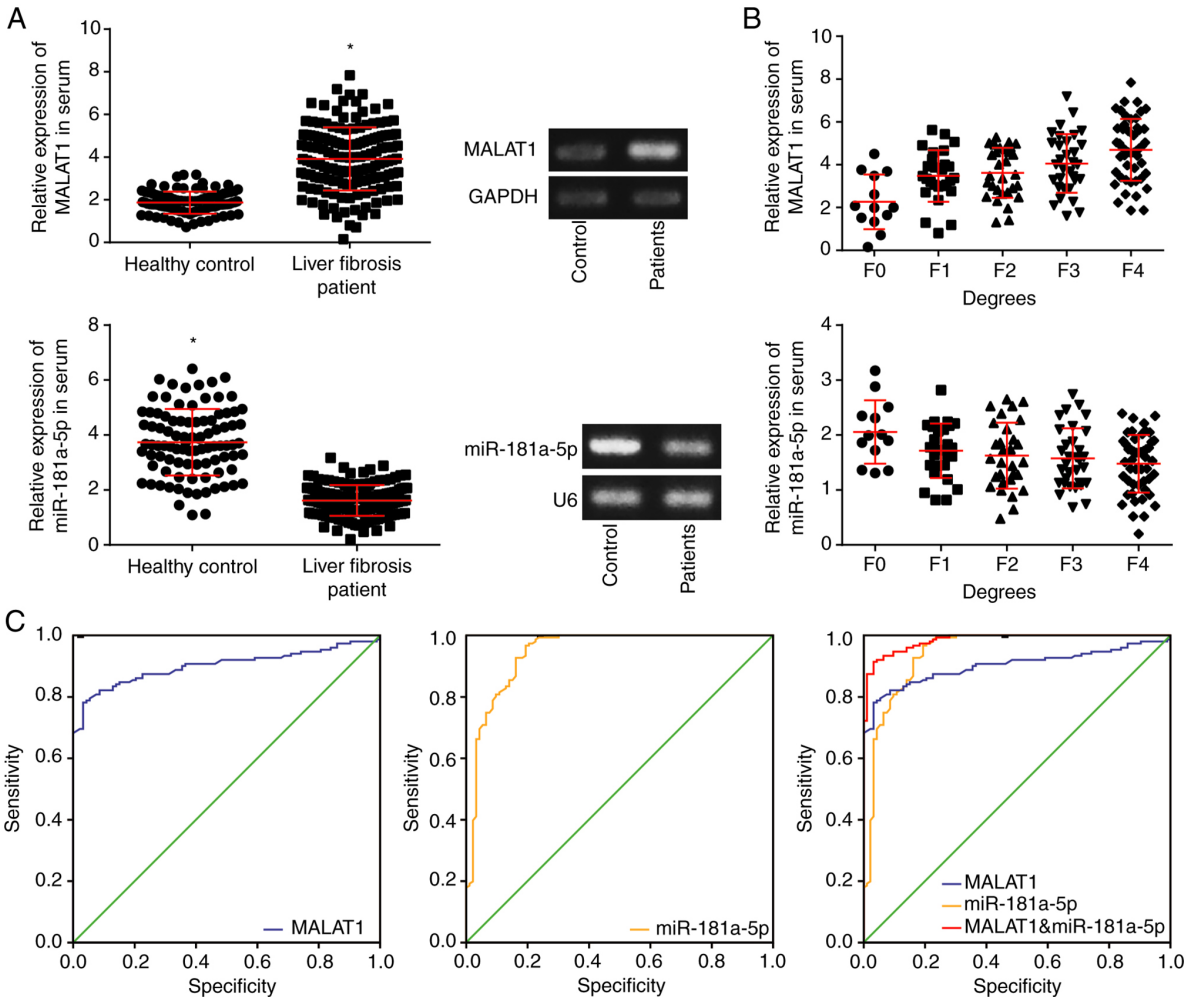

Figure 1. Clinical significance of lncRNA MALAT1 and miR-181a-5p in liver fibrosis. (A) Serum levels of MALAT1 and miR-181a-5p were compared between patients with liver fibrosis and healthy volunteers. *P<0.05 compared with healthy volunteers. (B) Serum levels of lncRNA MALAT1 and miR-181a-5p were determined in patients with stage F0, F1, F2, F3 or F4 liver fibrosis. (C) Diagnostic efficacy of MALAT1 and miR-181a-5p for liver fibrosis. lncRNA MALAT1, long non-coding RNA metastasis associated lung adenocarcinoma transcript 1; miR, microRNA.

of TLR4 and NF-κB were increased in LX2 cells transfected with pcDNA3.1-MALAT1 (P<0.05), whereas transfection of pcDNA3.1-MALAT1+miR-181a-5p mimic counteracted this increase (P<0.05; Fig. 4D).

MALAT1 promotes collagen production, viability, proliferation, migration and adhesion of HSCs. LX2 cells exposed to 5, 10 and 15 ng/ml TGF-β1 all expressed higher levels of MALAT1 and lower levels of miR-181a-5p than the control group (P<0.05; Fig. 5A). Additionally, 5 ng/ml TGF-β1 significantly increased the expression of TLR4 and NF-κB compared with the control group (P<0.05; Fig. 5A). In the presence of TGF-β1, TLR4 and NF-κB expression were significantly increased by transfection of pcDNA3.1-MALAT1 and were significantly suppressed by transfection of si-MALAT1, compared with TGF-β1 alone (P<0.05). Moreover, expression of α-SMA, COL1 and TIMP-1 were increased in LX2 cells upon stimulation with 5 ng/ml TGF-β1 (P<0.05), and they were increased further by simultaneous transfection with pcDNA3.1-MALAT1 (P<0.05; Fig. 5C).

Viability (Fig. 5D) and proliferation (Fig. 5E) of LX2 cells were increased, and the apoptotic rate decreased (Fig. 5F) following TGF-β1 treatment (P<0.05). Transfection

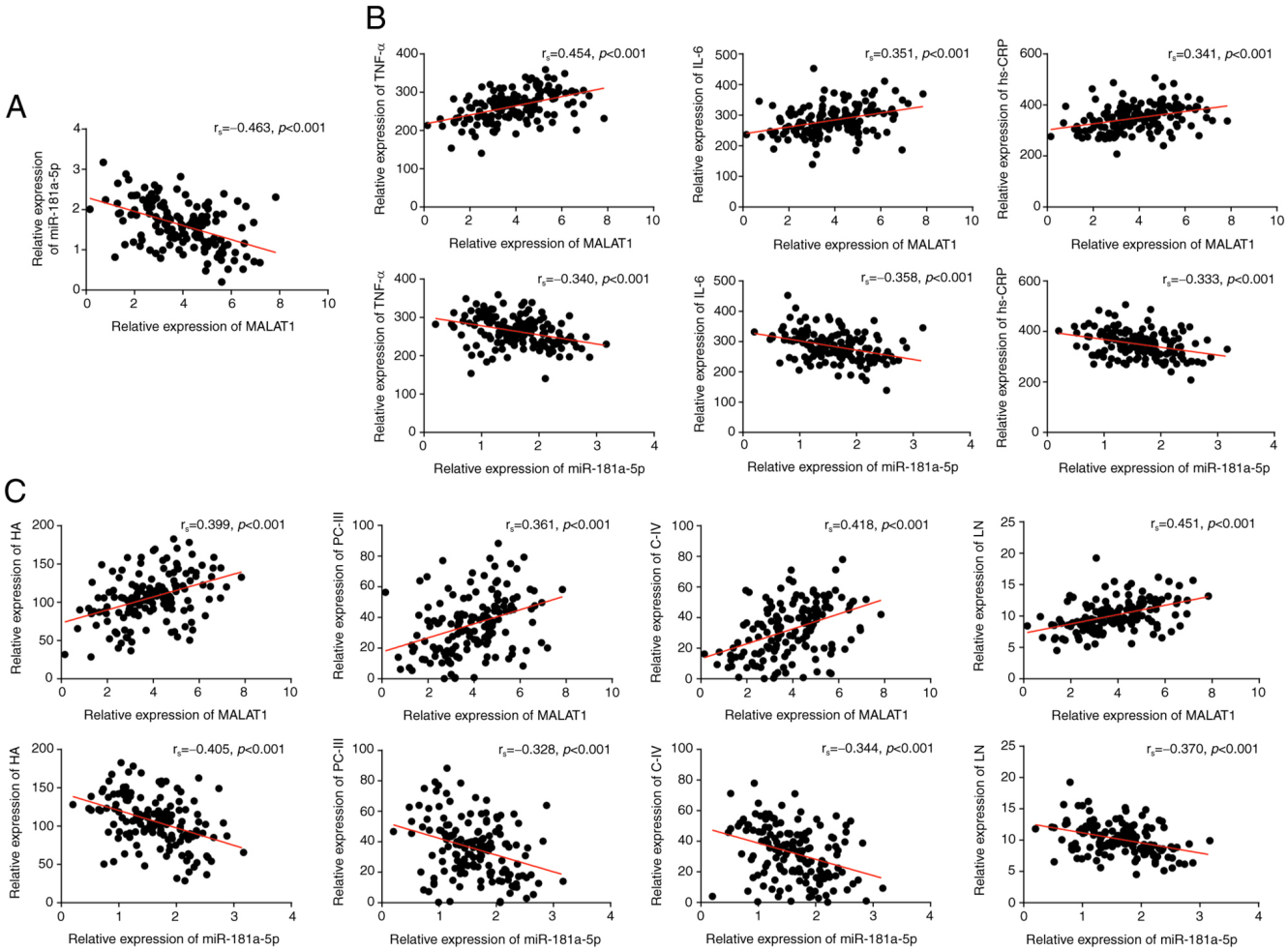

Figure 2. Correlation between serum levels of lncRNA MALAT1/miR-181a-5p and liver fibrosis indicators. (A) Serum MALAT1 levels were negatively correlated with miR-181a-5p levels amongst patients with liver fibrosis. (B) MALAT1/miR-181a-5p levels were associated with the levels of inflammatory cytokines in the patients with liver fibrosis. (C) MALAT1 and miR-181a-5p levels were associated with the quantity of liver fibrosis indicators amongst the patients with liver fibrosis. lncRNA MALAT1, long non-coding RNA metastasis associated lung adenocarcinoma transcript 1; miR, microRNA.

of pcDNA3.1-MALAT1 in the presence of TGF-β1 increased viability and proliferation, and decreased apoptosis, even further than TGF-β1 alone (all P<0.05). In contrast, transfection with si-MALAT1 in the presence of TGF-β1 decreased viability and proliferation, and increased apoptosis compared with TGF-β1 alone (P<0.05). Bax and cleaved caspase-3 expression were decreased, and Bcl-2 expression was increased by transfection with pcDNA3.1-MALAT1 in the presence of TGF-β1, when compared with TGF-β1 alone (P<0.05; Fig. 5G). In contrast, Bax and cleaved caspase-3 levels were upregulated, and Bcl-2 was downregulated following si-MALAT1 transfection in the presence of TGF-β1, compared with TGF-β1 alone (P<0.05). Migration and adhesion of TGF-β1-treated LX2 cells were increased by pcDNA3.1-MALAT1 transfection (P<0.05), and reduced by si-MALAT1 transfection (P<0.05; Fig. 6A and B). Transfection of LX2 cells with pcDNA3.1-MALAT1 in the presence of TGF-β1 increased Desmin and Vimentin expression, and decreased E-cadherin expression, compared with TGF-β1 alone (all P<0.05). In contrast, transfection with si-MALAT1 in the presence of TGF-β1 upregulated E-cadherin, and downregulated Desmin and Vimentin, compared with TGF-β1 alone (P<0.05; Fig. 6C).

miR-181a-5p inhibits collagen production and reduces viability, proliferation, migration and adhesion of HSCs. Expression of TLR4, NF-κB, α-SMA, COL1 and TIMP-1 were significantly increased following transfection of miR-181a-5p inhibitor in the presence of TGF-β1 (all P<0.05), whereas they were markedly reduced by transfection of miR-181a-5p mimic, compared to TGF-β1 alone (all P<0.05; Fig. 7A and B). In the presence of TGF-β1, viability and proliferation of LX2 cells was increased by transfection with miR-181a-5p inhibitor (both P<0.05), and decreased by transfection with miR-181a-5p mimic (both P<0.05), when compared with TGF-β1 alone (Fig. 7C and D). Conversely, the apoptotic rate of LX2 cells was increased by transfection with miR-181a-5p mimic and decreased by transfection with miR-181a-5p inhibitor, compared with TGF-β1 alone (all P<0.05; Fig. 7E). In concordance with these data, Bax and cleaved caspase-3 expression were reduced, and Bcl-2 expression was increased following miR-181a-5p inhibitor transfection, and *vice versa* for miR-181a-5p mimic transfection (all P<0.05; Fig. 7F).

In the presence of TGF-β1, migration and adhesion of LX2 cells was significantly increased by miR-181a-5p inhibitor transfection, and decreased by miR-181a-5p mimic transfection (all P<0.05) (Fig. 8A and B). Expression of Desmin and

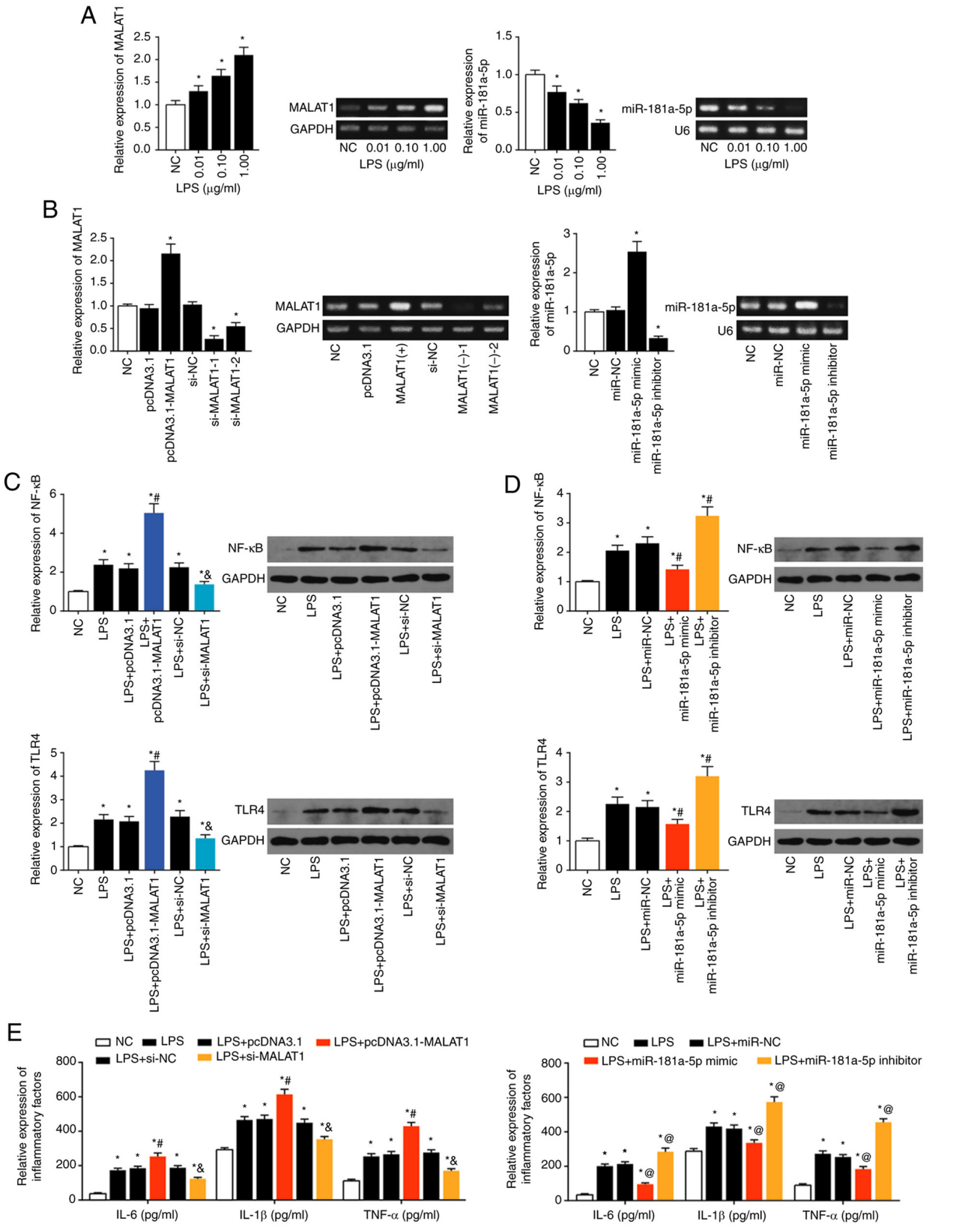

Figure 3. Effect of the lncRNA MALAT1/miR-181a-5p axis on NF-κB/TLR4 signaling. (A) MALAT1 and miR-181a-5p expressions were determined in LX2 cells with different concentrations of LPS. *P<0.05 vs. NC. (B) MALAT1 and miR-181a-5p expression was assessed after transfection of pcDNA3.1-MALAT1, si-MALAT1-1, si-MALAT1-2, miR-181a-5p mimic and miR-181a-5p inhibitor. *P<0.05 vs. NC. (C) NF-κB and TLR4 expression levels were detected in the LX2 cells treated with LPS, LPS+pcDNA3.1, LPS+pcDNA3.1-MALAT1, LPS+si-NC and LPS+si-MALAT1. *P<0.05 vs. NC; #P<0.05 vs. LPS+pcDNA3.1; &P<0.05 vs. LPS+si-NC. (D) NF-κB and TLR4 expression levels were compared in the LX2 cells treated with, LPS, LPS+miR-NC, LPS+miR-181a-5p mimic and LPS+miR-181a-5p inhibitor. *P<0.05 vs. NC; #P<0.05 vs. LPS+miR-NC. (E) The levels of inflammatory cytokines were assessed in LX2 cells treated with LPS, LPS+pcDNA3.1, LPS+pcDNA3.1-MALAT1, LPS+si-NC and LPS+si-MALAT1 as well as, LPS+miR-NC, LPS+miR-181a-5p mimic and LPS+miR-181a-5p inhibitor. *P<0.05 vs. NC; #P<0.05 vs. LPS+pcDNA3.1; &P<0.05 vs. LPS+si-NC; @P<0.05 vs. miR-NC. lncRNA MALAT1, long non-coding RNA metastasis associated lung adenocarcinoma transcript 1; miR, microRNA; NF-κB, nuclear factor-κB; TLR4, toll-like receptor-4; LPS, lipopolysaccharide; siRNA, small interfering RNA; NC, negative control.

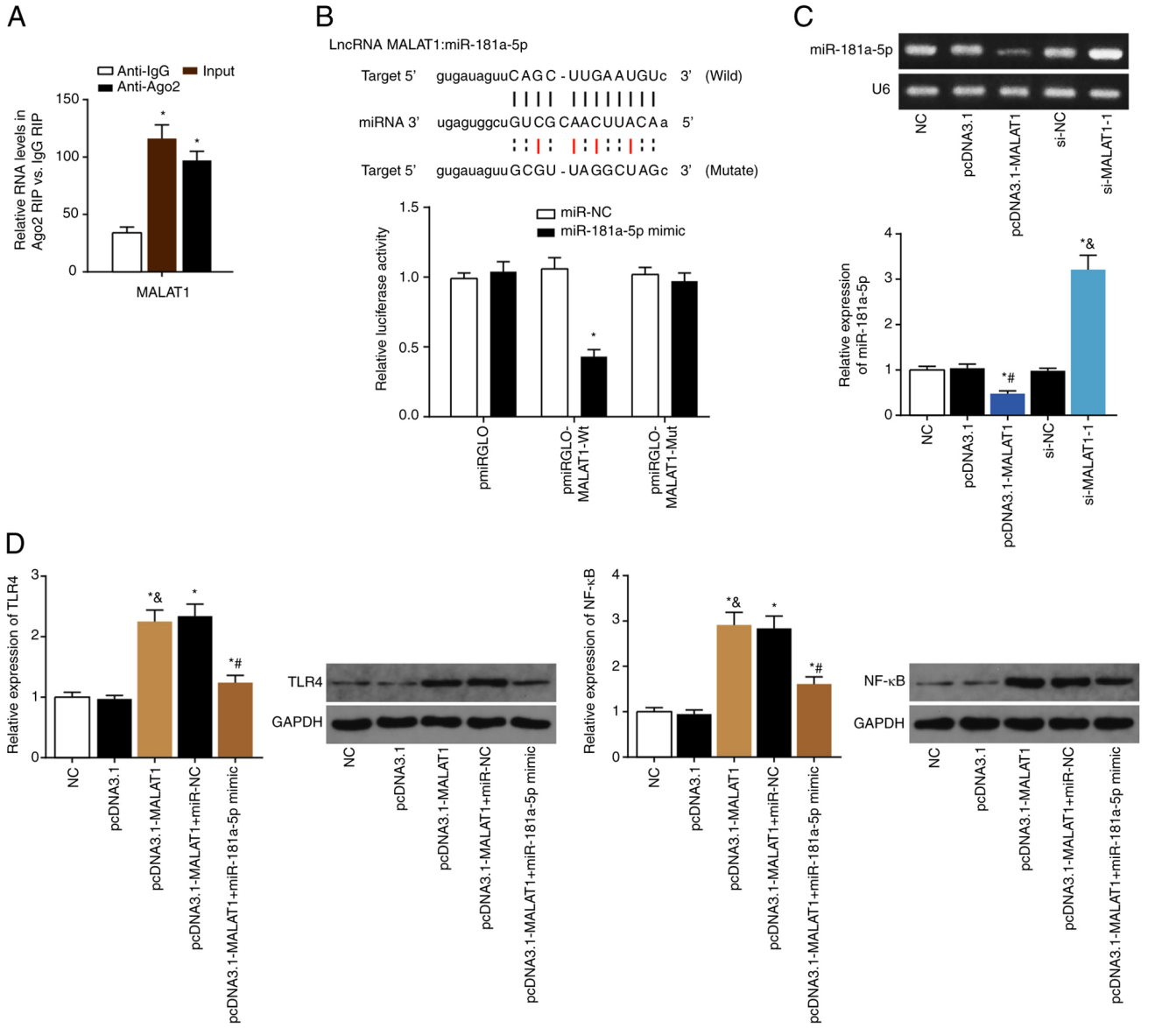

Figure 4. Sponging relationship between MALAT1 and miR-181a-5p in LX2 cells. (A) RNA immunoprecipitation assay was performed in LX2 cell lysates with antibodies against Ago2/IgG, and expression of MALAT1 was detected via PCR. (B) Luciferase activity of LX2 cells was compared between the pmiRGLO-MALAT1-Wt+miR-181a-5p mimic group and pmiRGLO-MALAT1-Wt+miR-NC group. *P<0.05 vs. pmiRGLO-MALAT1-Wt+miR-NC. (C) miR-181a-5p expression was determined in LX2 cells treated with pcDNA3.1, pcDNA3.1-MALAT1, si-NC and si-MALAT1-1. *P<0.05 vs. NC; #P<0.05 vs. pcDNA3.1; &P<0.05 vs. si-NC. (D) NF-κB and TLR4 expression levels in LX2 cells transfected with pcDNA3.1, pcDNA3.1-MALAT1, pcDNA3.1-MALAT1+miR-NC or pcDNA3.1-MALAT1+miR-181a-5p mimic. *P<0.05 vs. NC; #P<0.05 vs. pcDNA3.1-MALAT1+miR-NC; &P<0.05 vs. pcDNA3.1. MALAT1, metastasis associated lung adenocarcinoma transcript 1; miR, microRNA; NF-κB, nuclear factor-κB; TLR4, toll-like receptor-4; siRNA, small interfering RNA; NC, negative control.

Vimentin were decreased and expression of E-cadherin was increased following miR-181a-5p inhibitor transfection (all P<0.05), and *vice versa* for miR-181a-5p mimic transfection, compared with TGF-β1 alone (P<0.05; Fig. 8C).

Discussion

Several studies have highlighted the importance of TLR4/NF-κB signaling for the induction of liver fibrosis (20). Activation of NF-κB signaling inhibits apoptosis of HSCs, and enables HSCs to maintain a continuously-activated state (21). LPS-activated TLR4/NF-κB signaling led to the release of inflammatory factors (such as IL-8) and adhesion molecules (such as monocyte chemoattractant protein-1), both of which are markers of liver fibrosis (22-24). Following binding to receptors on the HSC surface, the TLR4/NF-κB axis participates in phosphorylation of Smad, thereby triggering secretion of collagen, whose deposition contributes to liver fibrosis progression (9,10). Given the importance of TLR4/NF-κB signaling in liver fibrosis, upstream molecules that modulate this pathway are worthy of intensive exploration.

In the present study, lncRNA MALAT1, initially identified in non-small cell lung cancer in 2003 (25), was found to promote TLR4 and NF-κB expression in an HSC cell line, thus not only increasing TGF-β1-induced proliferation, migration and adhesion, but also exacerbating LPS-triggered release of inflammatory cytokines (including IL-6, IL-1β and TNF-α) and collagen synthesis. It has been

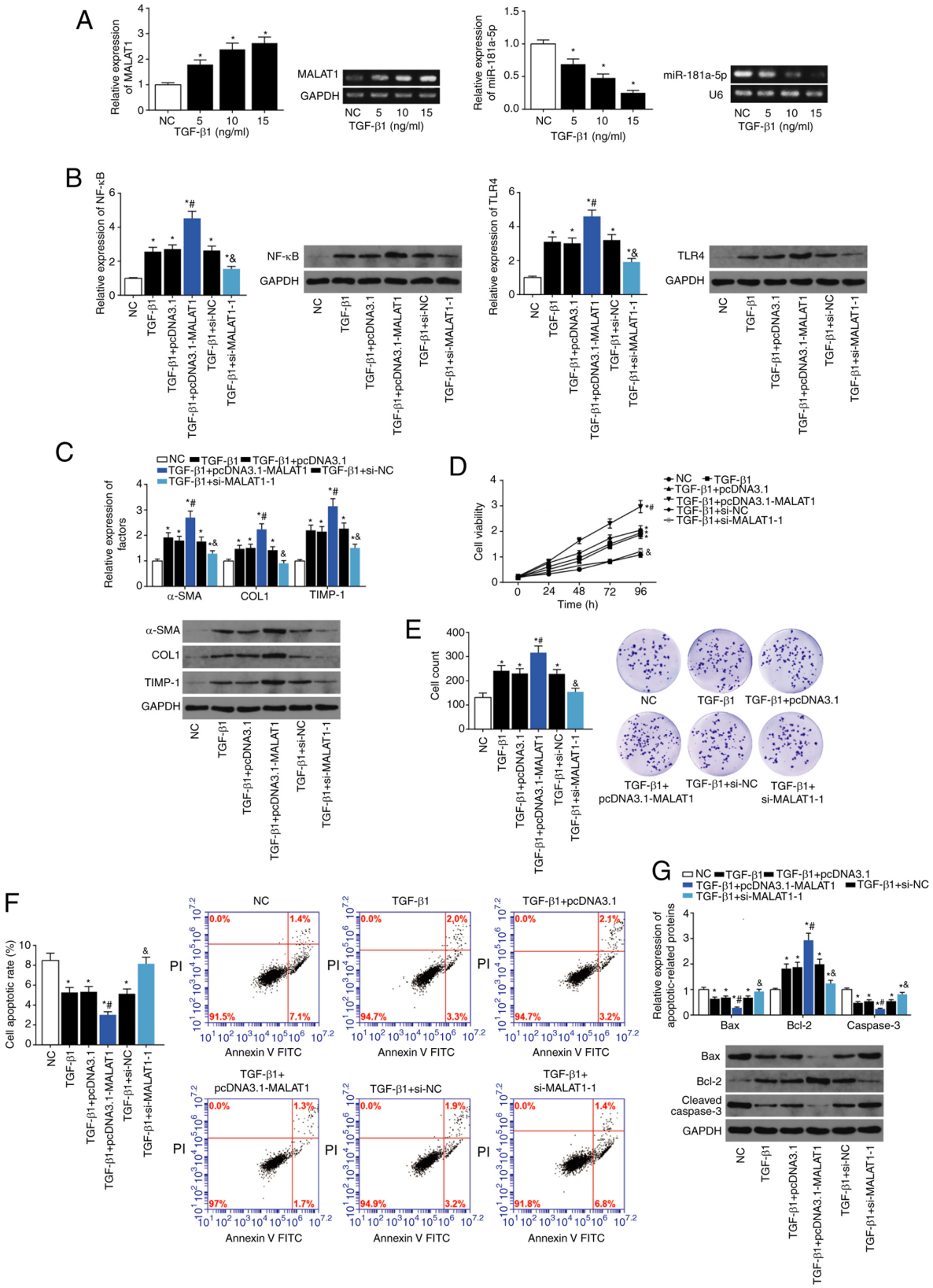

Figure 5. Impact of lncRNA MALAT1 on the viability and proliferation of LX2 cells. (A) Expression levels of MALAT1 and miR-181a-5p were estimated in LX2 cells treated with different concentrations of TGF-β1. *P<0.05 vs. NC. (B) Expression levels of NF-κB and TLR4 were detected in LX2 cells treated with NC, TGF-β1, TGF-β1+pcDNA3.1, TGF-β1+pcDNA3.1-MALAT1, TGF-β1+si-NC and TGF-β1+si-MALAT1. *P<0.05 vs. NC; #P<0.05 vs. TGF-β1+pcDNA3.1; &P<0.05 vs. TGF-β1+si-NC. (C) α-SMA, COL1 and TIMP-1 levels were evaluated in LX2 treated with TGF-β1, TGF-β1+pcDNA3.1, TGF-β1+pcDNA3.1-MALAT1, TGF-β1+si-NC and TGF-β1+si-MALAT1. *P<0.05 vs. NC; #P<0.05 vs. TGF-β1+pcDNA3.1; &P<0.05 vs. TGF-β1+si-NC. (D) Viability, (E) proliferation, (F) apoptosis and (G) apoptin expression were determined in the TGF-β1, TGF-β1+pcDNA3.1, TGF-β1+pcDNA3.1-MALAT1, TGF-β1+si-NC and TGF-β1+si-MALAT1 treated LX2 cells. *P<0.05 vs. NC; #P<0.05 vs. TGF-β1+pcDNA3.1; &P<0.05 vs. TGF-β1+si-NC. lncRNA MALAT1, long non-coding RNA metastasis associated lung adenocarcinoma transcript 1; miR, microRNA; NF-κB, nuclear factor-κB; TLR4, toll-like receptor-4; siRNA, small interfering RNA; NC, negative control; α-SMA, α-smooth muscle actin; COL1, collagen 1; TIMP-1, tissue inhibitor of metalloprotease-1; TGF-β1, transforming growth factor-β1.

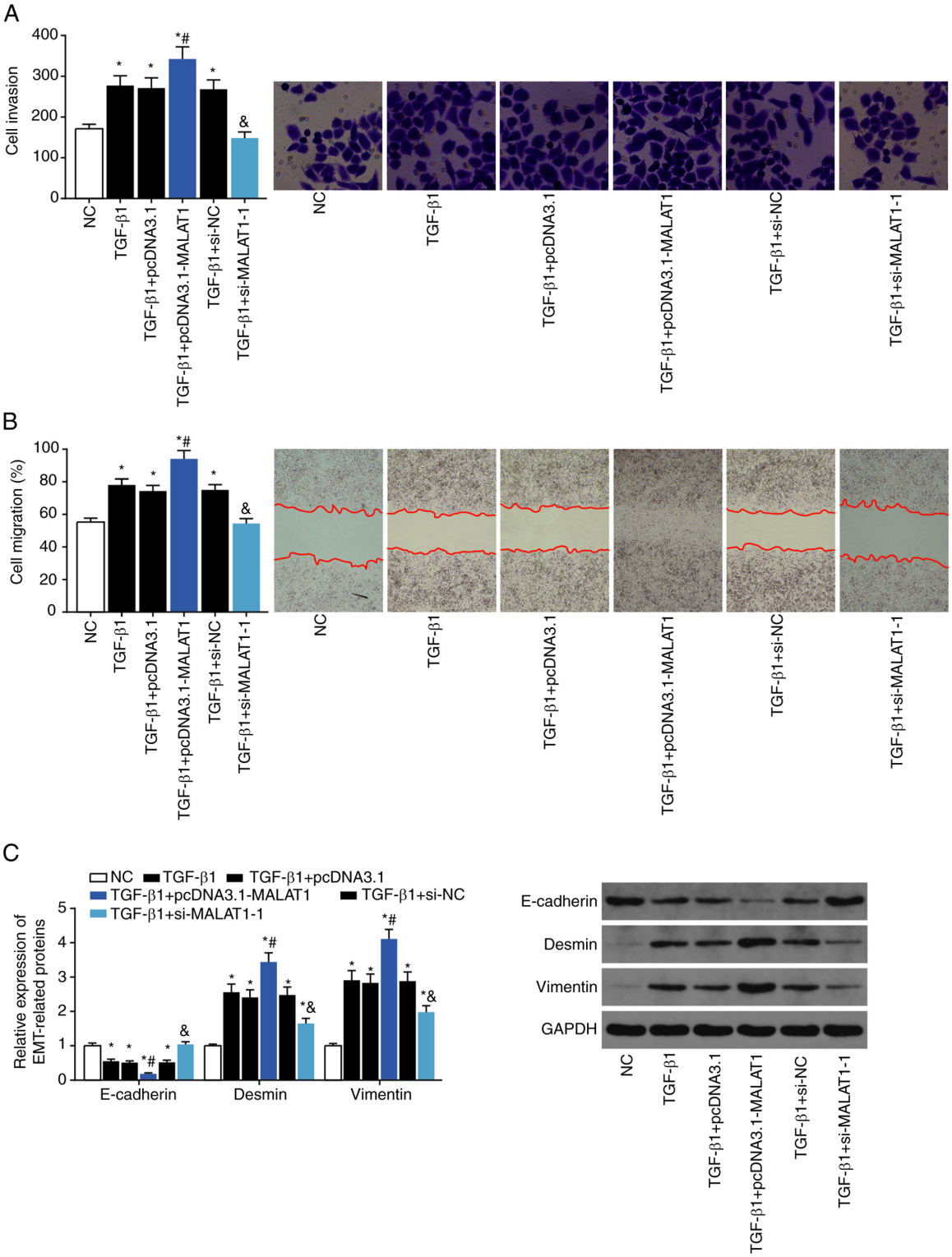

Figure 6. Impact of lncRNA MALAT1 on the migration and adhesion of LX2 cells. Expression of (A) migration, (B) adhesion and (C) epithelial-mesenchymal transition-associated proteins were determined in the LX2 cells treated with TGF-β1, TGF-β1+pcDNA3.1, TGF-β1+pcDNA3.1-MALAT1, TGF-β1+si-NC and TGF-β1+si-MALAT1. *P<0.05 vs. NC; #P<0.05 vs. TGF-β1+pcDNA3.1; &P<0.05 vs. TGF-β1+si-NC. TGF-β1, transforming growth factor-β1; MALAT1, metastasis associated lung adenocarcinoma transcript 1; miR, microRNA; siRNA, small interfering RNA; NC, negative control.

reported that MALAT1 regulates the malignant activity and inflammatory responses of several cell types. For example, knockout of MALAT1 reduced proliferation and migration of esophageal squamous cell carcinoma cells (26), and knock-down of MALAT1 led to G2/M arrest by compromising the cytoplasmic transfer of Heterogeneous nuclear ribonucleoproteins C (27), which all support the notion that MALAT1 enhanced migration and proliferation of cells, just as was observed in HSCs. MALAT1 has also been suggested to promote glucose induced secretion of inflammatory cytokines, such as TNF-α and IL-6, by activating SAA3 (28). However, one study reported that MALAT1 negatively

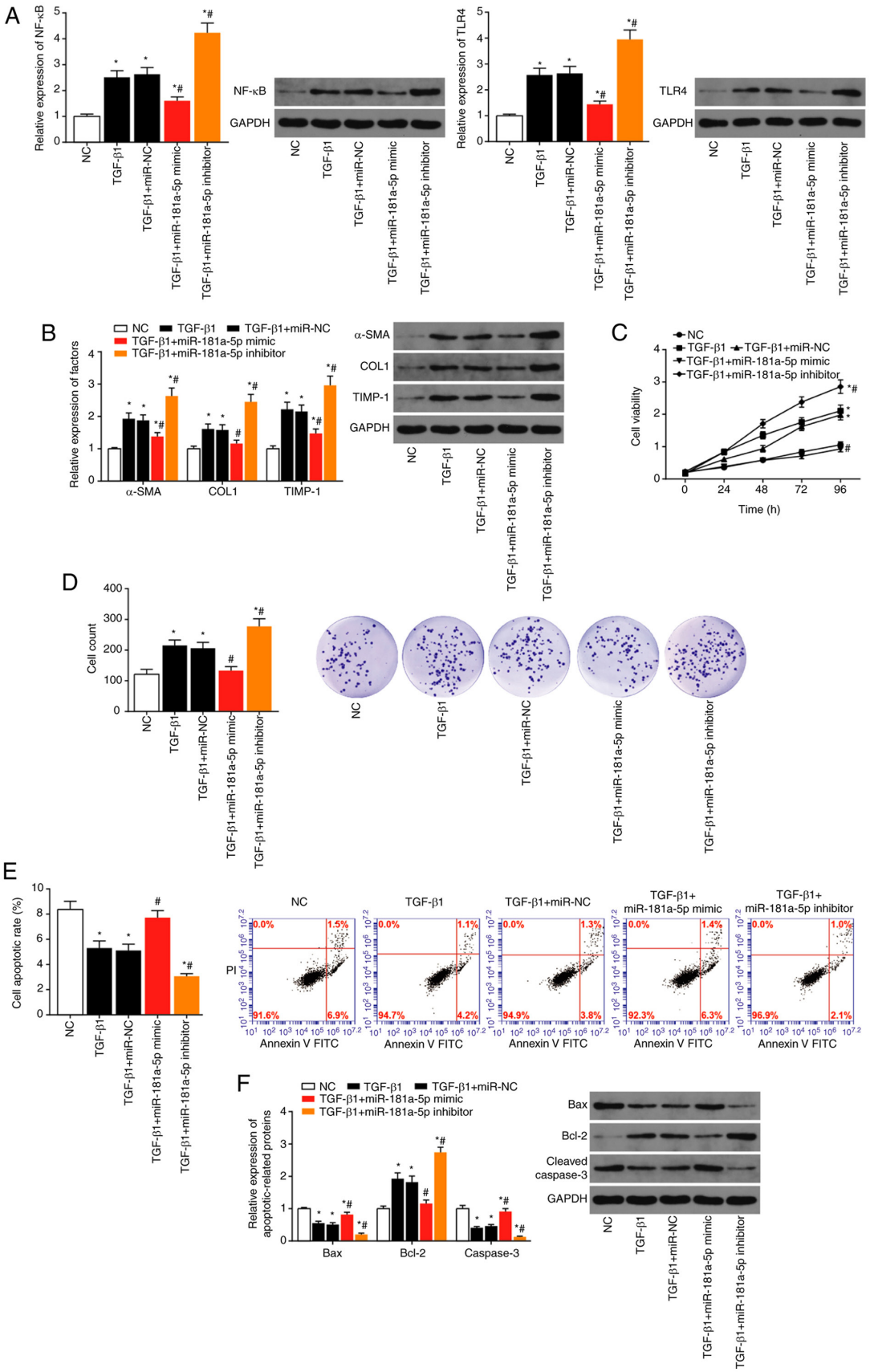

Figure 7. Effect of miR-181a-5p on the viability and proliferation of LX2 cells. (A) Expression levels of NF-κB and TLR4 were detected in LX2 cells treated with TGF-β1, TGF-β1+miR-NC, TGF-β1+miR-181a-5p mimic and TGF-β1+miR-181a-5p inhibitor. *P<0.05 vs. NC; #P<0.05 vs. TGF-β1+miR-NC. (B) The expression levels of α-SMA, COL1 and TIMP-1 were evaluated in the LX2 cells treated with TGF-β1, TGF-β1+miR-NC, TGF-β1+miR-181a-5p mimic and TGF-β1+miR-181a-5p inhibitor. *P<0.05 vs. NC; #P<0.05 vs. TGF-β1+miR-NC group. (C) Viability, (D) proliferation, (E) apoptosis activity as well as (F) apoptin expression in LX2 cells treated with TGF-β1, TGF-β1+miR-NC, TGF-β1+miR-181a-5p mimic and TGF-β1+miR-181a-5p inhibitor were determined. *P<0.05 vs. NC; #P<0.05 vs. TGF-β1+miR-NC. miR, microRNA; NC, negative control; NF-κB, nuclear factor-κB; TLR4, toll-like receptor-4; α-SMA, α-smooth muscle actin; COL1, collagen 1; TIMP-1, tissue inhibitor of metalloprotease-1; TGF-β1, transforming growth factor-β1.

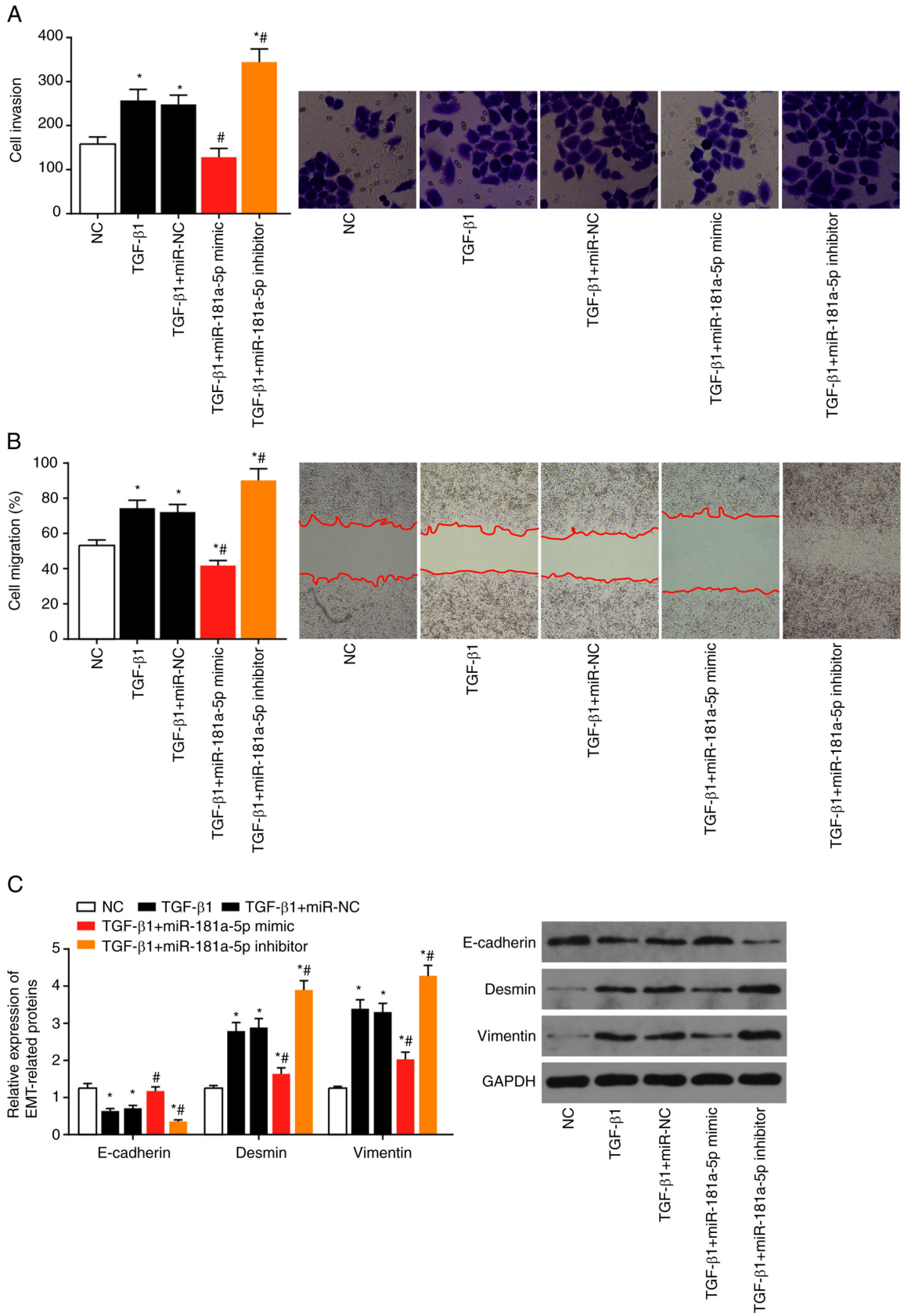

Figure 8. Effect of miR-181a-5p on the migration and adhesion of LX2 cells. Expression of (A) migration, (B) adhesion and (C) epithelial-mesenchymal transition-associated proteins were determined in the LX2 cells treated with TGF-β1, TGF-β1+miR-NC, TGF-β1+miR-181a-5p mimic and TGF-β1+miR-181a-5p inhibitor. *P<0.05 vs. NC; #P<0.05 vs. TGF-β1+miR-NC. NC, negative control; miR, microRNA; TGF-β1, transforming growth factor-β1.

regulated NF-κB and thereby inhibited the release of inflammatory cytokines from LPS-activated macrophages (29), which does not agree with the results of the present study. It is possible that the influence of MALAT1 on inflammation

varies between cell types, and that MALAT1 may perform distinct functions in different disorders.

In agreement with the competing endogenous RNA hypothesis, it was further shown that miR-181a was sponged and downregulated by MALAT1 in HSCs. It was previously reported that TGF-β1, which facilitates liver fibrosis by activating HSCs and driving synthesis of extracellular matrix proteins (such as type I/III collagen) (30), promoted shear maturation of pri-miR-181a through activation of Smad2/3 and the Drosha miRNA processing complex (31). Moreover, TGF-β also induced high levels of precursor and mature miR-181 in hepatic cells by targeting and controlling TIMP3 expression (32). Here, it was proposed that TGF-β may downregulate miR-181 expression in HSCs by increasing MALAT1 expression, and that the MALAT1/miR-181a axis may be involved in TGF-β-mediated HSC activation. In agreement with the HSC data in the present study, miR-181a was reported to reduce proliferation and migration of cutaneous squamous cell carcinoma cells (33), oral squamous cell carcinoma cells (34), non-small cell lung cancer cells (35) and malignant glioma cells (36). However, miR-181a appeared to facilitate oncogenesis in breast cancer (37) and liver cancer (38). To explain this seeming contradiction, it is speculated that there may be additional mechanisms yet to be discovered, such as bi-directional regulation in breast cancer (39), and that miR-181a could exert different effects in different diseases. miR-181a was reported to regulate the development of embryonic organs, the lymphatic system and blood cell lines (40), as well as the differentiation of megakaryocytes and maturation of T lymphocytes (41). Consistent with an earlier study that reported downregulation of miR-181a in a LPS-induced ALI rat model (42), it was shown in the present study that miR-181a repressed inflammation in HSCs by deactivation of the TLR4/NF-κB axis. Together, the results of the present study showed that miR-181a was pivotal for the contribution of MALAT1 to the activation and inflammation of the LX2 cell line.

In conclusion, inflammation and HSC activation were of significance to the development of liver fibrosis (43,44). TGF-β1 is typically used to induce HSC activation and proliferation (45). LPS, a constituent of the cell wall of gram-negative bacteria, elicits a series of inflammation responses, and is often applied to establish cell models of inflammation in the study of liver fibrosis (46). This investigation used TGF-β1 to trigger HSC activation and utilized LPS to construct models of inflammation of HSC. In both cell models, a MALAT1/miR181a/TLR4/NF-κB axis was studied, and an association of MALAT1/miR181a/TLR4/NF-κB axis with HSC activation and inflammation was identified. There are several potential shortcomings in the experimental design used. Firstly, the liver fibrosis cohort were all HBV-infected, so it is unclear whether the MALAT1-miR-181-TLR4/NF-kB axis behaves similarly in cases of non-HBV liver fibrosis. Secondly, only a single cell line was included; the data would be more convincing if other cell lines or primary cells were also studied. In future studies, these mentioned limitations will be addressed and animal models of liver fibrosis will be used to verify these findings *in vitro*, which will provide support for the proposed model of the role of the MALAT1/miR-181 axis in liver fibrosis.

Acknowledgements

Not applicable.

Funding

This study was financially supported by the Qian ke he platform talents [grant no. (2018)5779-26].

Availability of data and materials

The datasets used and/or analyzed during the present study are available from the corresponding author on reasonable request.

Authors' contributions

YW, QM, ZZ, LuZ and LiZ conceived and designed the experiments. YW, QM and ZZ performed the experiments. ZZ analyzed the data. LuZ and LiZ drafted the manuscript. YW and QM confirm the authenticity of all the raw data. All authors read and approved the final manuscript.

Ethics approval and consent to participate

The present study was approved by the Ethics Committee of the Affiliated Hospital of Guizhou Medical University. Written informed consent was obtained from all participants included in the present study.

Patient consent for publication

Not applicable.

Competing interests

The authors declare that they have no competing interests.

References

1. Yin C, Evason KJ, Asahina K and Stainier DY: Hepatic stellate cells in liver development, regeneration, and cancer. J Clin Invest 123: 1902-1910, 2013.
2. Higashi T, Friedman SL and Hoshida Y: Hepatic stellate cells as key target in liver fibrosis. Adv Drug Deliv Rev 121: 27-42, 2017.
3. Dixon LJ, Barnes M, Tang H, Pritchard MT and Nagy LE: Kupffer cells in the liver. Compr Physiol 3: 785-797, 2013.
4. Koyama Y and Brenner DA: Liver inflammation and fibrosis. J Clin Invest 127: 55-64, 2017.
5. Dhar D, Baglieri J, Kisseleva T and Brenner DA: Mechanisms of liver fibrosis and its role in liver cancer. Exp Biol Med (Maywood) 245: 96-108, 2020.
6. Peng H, Wan LY, Liang JJ, Zhang YQ, Ai WB and Wu JF: The roles of lncRNA in hepatic fibrosis. Cell Biosci 8: 63, 2018.
7. Zhang K, Han X, Zhang Z, Zheng L, Hu Z, Yao Q, Cui H, Shu G, Si M, Li C, *et al*: The liver-enriched lnc-LFAR1 promotes liver fibrosis by activating TGFβ and Notch pathways. Nat Commun 8: 144, 2017.
8. Wang X, Cheng Z, Dai L, Jiang T, Jia L, Jing X, An L, Wang H and Liu M: Knockdown of long noncoding RNA H19 represses the progress of pulmonary fibrosis through the transforming growth factor β/smad3 pathway by regulating MicroRNA 140. Mol Cell Biol 39: e00143-19, 2019.
9. Dooley S and ten Dijke P: TGF-β in progression of liver disease. Cell Tissue Res 347: 245-256, 2012.
10. Yang JW, Hien TT, Lim SC, Jun DW, Choi HS, Yoon JH, Cho IJ and Kang KW: Pin1 induction in the fibrotic liver and its roles in TGF-β1 expression and Smad2/3 phosphorylation. J Hepatol 60: 1235-1241, 2014.

11. Wu Y, Liu X, Zhou Q, Huang C, Meng X, Xu F and Li J: Silent information regulator 1 (SIRT1) ameliorates liver fibrosis via promoting activated stellate cell apoptosis and reversion. Toxicol Appl Pharmacol 289: 163-176, 2015.
12. Jiang R, Zhou Y, Wang S, Pang N, Huang Y, Ye M, Wan T, Qiu Y, Pei L, Jiang X, *et al*: Nicotinamide riboside protects against liver fibrosis induced by CCl_4 via regulating the acetylation of smads signaling pathway. Life Sci 225: 20-28, 2019.
13. Yu F, Lu Z, Cai J, Huang K, Chen B, Li G, Dong P and Zheng J: MALAT1 functions as a competing endogenous RNA to mediate Rac1 expression by sequestering miR-101b in liver fibrosis. Cell Cycle 14: 3885-3896, 2015.
14. Dai X, Chen C, Xue J, Xiao T, Mostofa G, Wang D, Chen X, Xu H, Sun Q, Li J, *et al*: Exosomal MALAT1 derived from hepatic cells is involved in the activation of hepatic stellate cells via miRNA-26b in fibrosis induced by arsenite. Toxicol Lett 316: 73-84, 2019.
15. Sun Y, Jiang T, Jia Y, Zou J, Wang X and Gu W: LncRNA MALAT1/miR-181a-5p affects the proliferation and adhesion of myeloma cells via regulation of Hippo-YAP signaling pathway. Cell Cycle 18: 2509-2523, 2019.
16. Jiang K, Guo S, Zhang T, Yang Y, Zhao G, Shaukat A, Wu H and Deng G: Downregulation of TLR4 by miR-181a provides negative feedback regulation to lipopolysaccharide-induced inflammation. Front Pharmacol 9: 142, 2018.
17. Sahin H, Borkham-Kamphorst E, do O NT, Berres ML, Kaldenbach M, Schmitz P, Weiskirchen R, Liedtke C, Streetz KL, Maedler K, *et al*: Proapoptotic effects of the chemokine, CXCL 10 are mediated by the noncognate receptor TLR4 in hepatocytes. Hepatology 57: 797-805, 2013.
18. Zhu D, He X, Duan Y, Chen J, Wang J, Sun X, Qian H, Feng J, Sun W, Xu F and Zhang L: Expression of microRNA-454 in TGF-β1-stimulated hepatic stellate cells and in mouse livers infected with Schistosoma japonicum. Parasit Vectors 7: 148, 2014.
19. Livak KJ and Schmittgen TD: Analysis of relative gene expression data using real-time quantitative PCR and the 2(-Delta Delta C(T)) method. Methods 25: 402-408, 2001.
20. Lai L, Chen Y, Tian X, Li X, Zhang X, Lei J, Bi Y, Fang B and Song X: Artesunate alleviates hepatic fibrosis induced by multiple pathogenic factors and inflammation through the inhibition of LPS/TLR4/NF-κB signaling pathway in rats. Eur J Pharmacol 765: 234-241, 2015.
21. Chen Z, Amro EM, Becker F, Hölzer M, Rasa SMM, Njeru SN, Han B, Di Sanzo S, Chen Y, Tang D, *et al*: Cohesin-mediated NF-κB signaling limits hematopoietic stem cell self-renewal in aging and inflammation. J Exp Med 216: 152-175, 2019.
22. Kobayashi K, Yoshioka T, Miyauchi J, Nakazawa A, Yamazaki S, Ono H, Tatsuno M, Iijima K, Takahashi C, Okada Y, *et al*: Monocyte chemoattractant protein-1 (MCP-1) as a potential therapeutic target and a noninvasive biomarker of liver fibrosis associated with transient myeloproliferative disorder in down syndrome. J Pediatr Hematol Oncol 39: e285-e289, 2017.
23. Zimmermann HW, Seidler S, Gassler N, Nattermann J, Luedde T, Trautwein C and Tacke F: Interleukin-8 is activated in patients with chronic liver diseases and associated with hepatic macrophage accumulation in human liver fibrosis. PLoS One 6: e21381, 2011.
24. Vespasiani-Gentilucci U, Carotti S, Perrone G, Mazzarelli C, Galati G, Onetti-Muda A, Picardi A and Morini S: Hepatic toll-like receptor 4 expression is associated with portal inflammation and fibrosis in patients with NAFLD. Liver Int 35: 569-581, 2015.
25. Ji P, Diederichs S, Wang W, Böing S, Metzger R, Schneider PM, Tidow N, Brandt B, Buerger H, Bulk E, *et al*: MALAT-1, a novel noncoding RNA, and thymosin beta4 predict metastasis and survival in early-stage non-small cell lung cancer. Oncogene 22: 8031-8041, 2003.
26. Wang X, Li M, Wang Z, Han S, Tang X, Ge Y, Zhou L, Zhou C, Yuan Q and Yang M: Silencing of long noncoding RNA MALAT1 by miR-101 and miR-217 inhibits proliferation, migration, and invasion of esophageal squamous cell carcinoma cells. J Biol Chem 290: 3925-3935, 2015.
27. Yang F, Yi F, Han X, Du Q and Liang Z: MALAT-1 interacts with hnRNP C in cell cycle regulation. FEBS Lett 587: 3175-3181, 2013.
28. Puthanveetil P, Chen S, Feng B, Gautam A and Chakrabarti S: Long non-coding RNA MALAT1 regulates hyperglycaemia induced inflammatory process in the endothelial cells. J Cell Mol Med 19: 1418-1425, 2015.
29. Zhao G, Su Z, Song D, Mao Y and Mao X: The long noncoding RNA MALAT1 regulates the lipopolysaccharide-induced inflammatory response through its interaction with NF-κB. FEBS Lett 590: 2884-2895, 2016.
30. Liu N, Feng J, Lu X, Yao Z, Liu Q, Lv Y, Han Y, Deng J and Zhou Y: Isorhamnetin inhibits liver fibrosis by reducing autophagy and inhibiting extracellular matrix formation via the TGF-β1/smad3 and TGF-β1/p38 MAPK pathways. Mediators Inflamm 2019: 6175091, 2019.
31. Wang Y, Yu Y, Tsuyada A, Ren X, Wu X, Stubblefield K, Rankin-Gee EK and Wang SE: Transforming growth factor-β regulates the sphere-initiating stem cell-like feature in breast cancer through miRNA-181 and ATM. Oncogene 30: 1470-1480, 2011.
32. Wang B, Hsu SH, Majumder S, Kutay H, Huang W, Jacob ST and Ghoshal K: TGFbeta-mediated upregulation of hepatic miR-181b promotes hepatocarcinogenesis by targeting TIMP3. Oncogene 29: 1787-1797, 2010.
33. Neu J, Dziunycz PJ, Dzung A, Lefort K, Falke M, Denzler R, Freiberger SN, Iotzova-Weiss G, Kuzmanov A, Levesque MP, *et al*: miR-181a decelerates proliferation in cutaneous squamous cell carcinoma by targeting the proto-oncogene KRAS. PLoS One 12: e0185028, 2017.
34. Li GH, Ma ZH and Wang X: Long non-coding RNA CCAT1 is a prognostic biomarker for the progression of oral squamous cell carcinoma via miR-181a-mediated Wnt/β-catenin signaling pathway. Cell cycle 18: 2902-2913, 2019.
35. Shi Q, Zhou Z, Ye N, Chen Q, Zheng X and Fang M: MiR-181a inhibits non-small cell lung cancer cell proliferation by targeting CDK1. Cancer Biomark 20: 539-546, 2017.
36. Ma J, Yao Y, Wang P, Liu Y, Zhao L, Li Z, Li Z and Xue Y: MiR-181a regulates blood-tumor barrier permeability by targeting Krüppel-like factor 6. J Cereb Blood Flow Metab 34: 1826-1836, 2014.
37. Taylor MA, Sossey-Alaoui K, Thompson CL, Danielpour D and Schiemann WP: TGF-β upregulates miR-181a expression to promote breast cancer metastasis. J Clin Invest 123: 150-163, 2013.
38. Zhuang X, Chen Y, Wu Z, Xu Q, Chen M, Shao M, Cao X, Zhou Y, Xie M, Shi Y, *et al*: Mitochondrial miR-181a-5p promotes glucose metabolism reprogramming in liver cancer by regulating the electron transport chain. Carcinogenesis 41: 972-983, 2020.
39. Yang C, Tabatabaei SN, Ruan X and Hardy P: The dual regulatory role of MiR-181a in breast cancer. Cell Physiol Biochem 44: 843-856, 2017.
40. Seoudi AM, Lashine YA and Abdelaziz AI: MicroRNA-181a-a tale of discrepancies. Expert Rev Mol Med 14: e5, 2012.
41. Kim C, Jadhav RR, Gustafson CE, Smithey MJ, Hirsch AJ, Uhrlaub JL, Hildebrand WH, Nikolich-Žugich J, Weyand CM and Goronzy JJ: Defects in antiviral T cell responses inflicted by aging-associated miR-181a deficiency. Cell Rep 29: 2202-2216. e5, 2019.
42. Cai ZG, Zhang SM, Zhang Y, Zhou YY, Wu HB and Xu XP: MicroRNAs are dynamically regulated and play an important role in LPS-induced lung injury. Can J Physiol Pharmacol 90: 37-43, 2012.
43. Anthony B, Allen JT, Li YS and McManus DP: Hepatic stellate cells and parasite-induced liver fibrosis. Parasit Vectors 3: 60, 2010.
44. Parola M and Pinzani M: Liver fibrosis: Pathophysiology, pathogenetic targets and clinical issues. Mol Aspects Med 65: 37-55, 2019.
45. Mu M, Zuo S, Wu RM, Deng KS, Lu S, Zhu JJ, Zou GL, Yang J, Cheng ML and Zhao XK: Ferulic acid attenuates liver fibrosis and hepatic stellate cell activation via inhibition of TGF-β/Smad signaling pathway. Drug Des Devel Ther 12: 4107-4115, 2018.
46. Hu N, Wang C, Dai X, Zhou M, Gong L, Yu L, Peng C and Li Y: Phillygenin inhibits LPS-induced activation and inflammation of LX2 cells by TLR4/MyD88/NF-κB signaling pathway. J Ethnopharmacol 248: 112361, 2020.